



Design optimization and heat transfer characteristics of multilayer insulation structures for liquid hydrogen tanks

Hongyu Lv, Liang Chen^{*}, Ze Zhang, Shuangtao Chen, Yu Hou

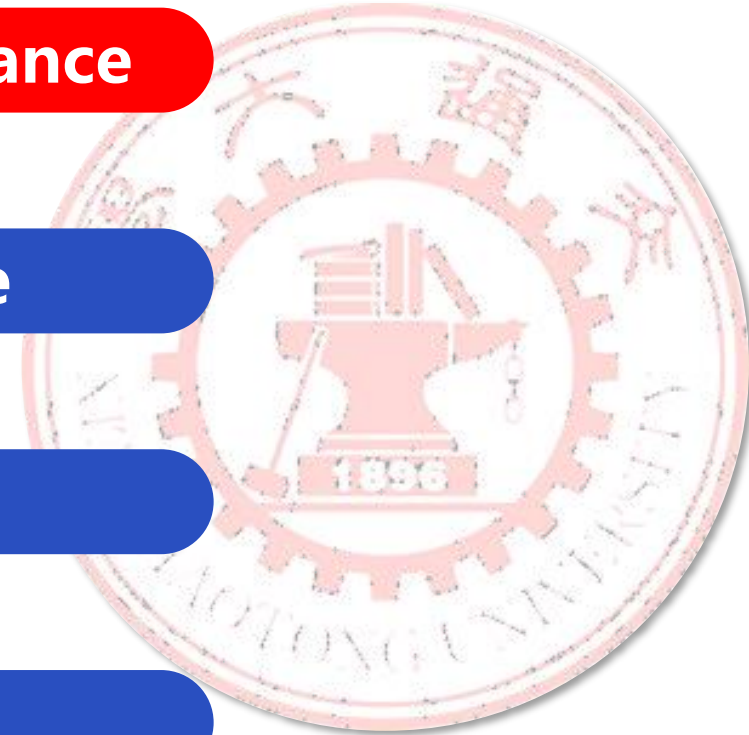
Reporter: Hongyu Lv

Institution: Xi' an Jiaotong University

Date: 2024. 07. 24

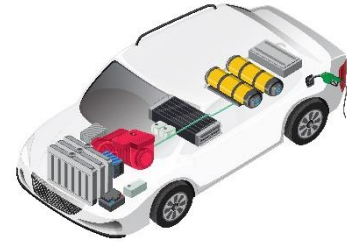
Content

- ① **Research background and significance**
- ② **Experimental system and principle**
- ③ **Results and discussions**
- ④ **Conclusions and Suggestions**



Hydrogen Energy:

- Zero release
- Renewability
- High energy density



Fuel cell



Aviation



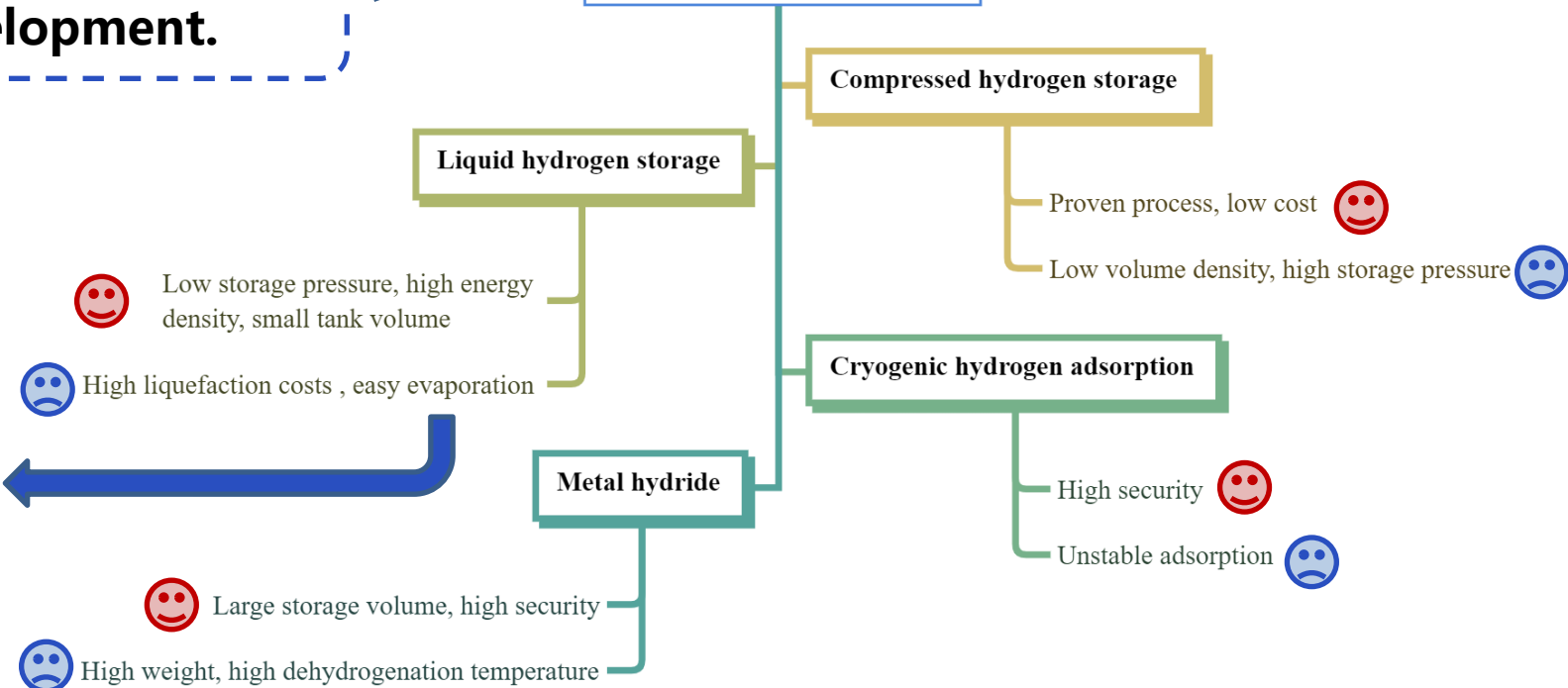
Electricity

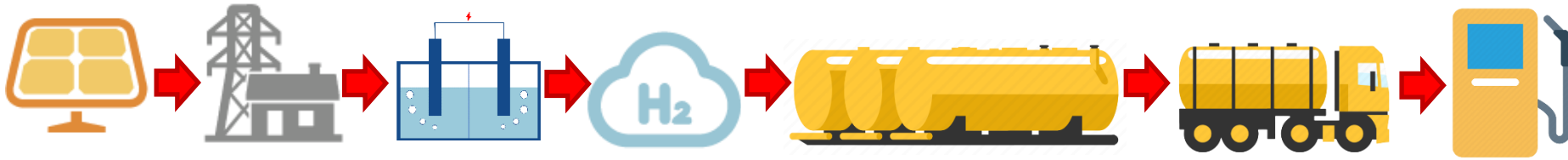
Suitable storage and transportation methods can facilitate the hydrogen energy development.

Liquid hydrogen

- ◆ Low boiling point (20.3 K)
- ◆ Low latent heat of vaporization (31.6 kJ/L)

Hydrogen storage method

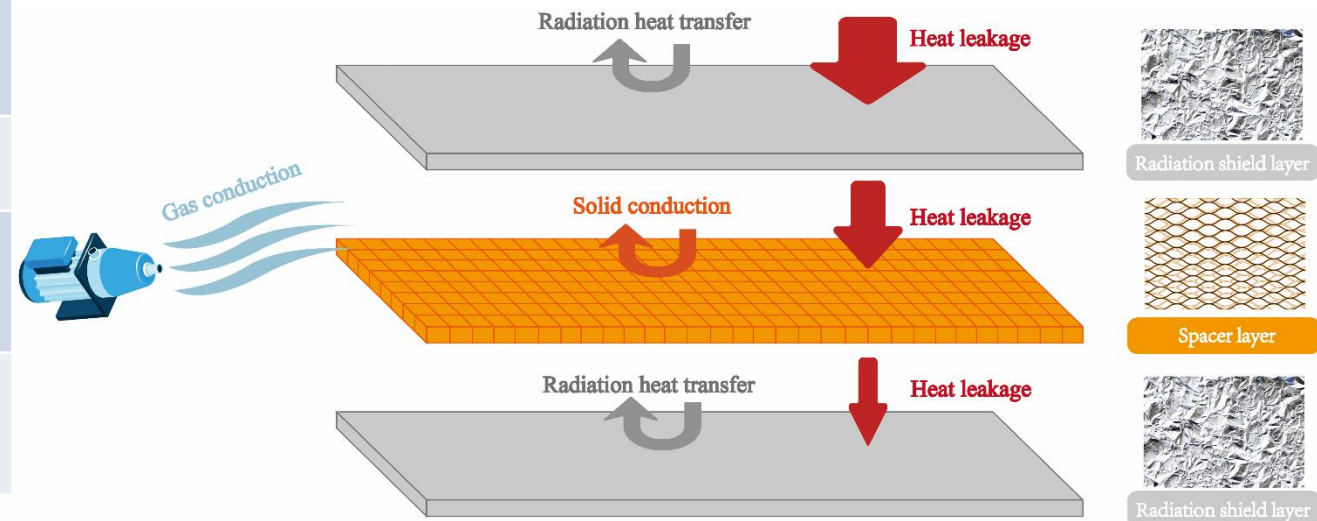
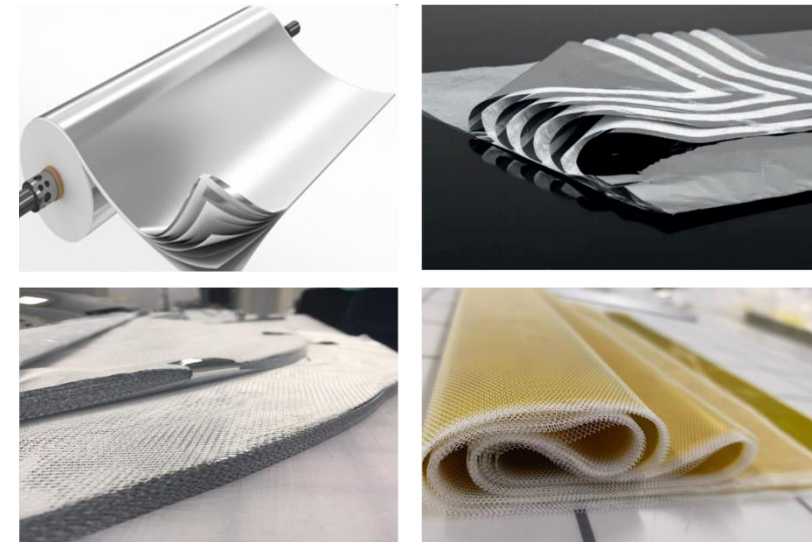




- ◆ **LH₂** is key to achieving **large-scaled** hydrogen storage
- ◆ **Low heat leakage**, highly compact LH₂ tanks

Reducing energy waste and improving safety

Insulation method	Insulation principle
Filling insulation	Reduce conductions by wrapping or packing low thermal conductivity foams, powders, and fibers around the interlayer.
High vacuum insulation	Vacuuming of the interlayer reduces convective heat transfer and gas conductivity.
Vacuum Powder Insulation	A low vacuum degree in the insulation interlayer based on filling insulation is maintained to eliminate gas conduction.
Vacuum multilayer insulation	Radiation shield layers parallel to the cryogenic container are added based on high vacuum insulation to reduce radiation heat transfer.



Main contents

Based on the multilayer insulation structure (MLI) performance experimental apparatus, the insulation properties of aluminum foil and glass fiber paper combined under the liquid nitrogen temperature zone are carried out.

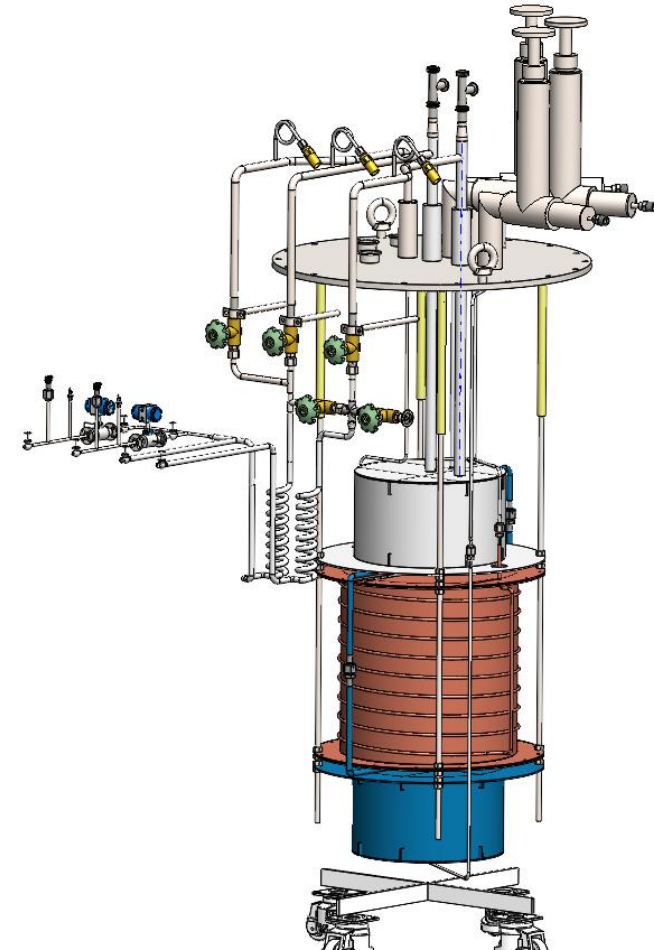
Experimental test

Investigate the effects of MLI layer density and layer number on the apparent thermal conductivity and heat flux at different warm boundary temperatures.

Performance analysis

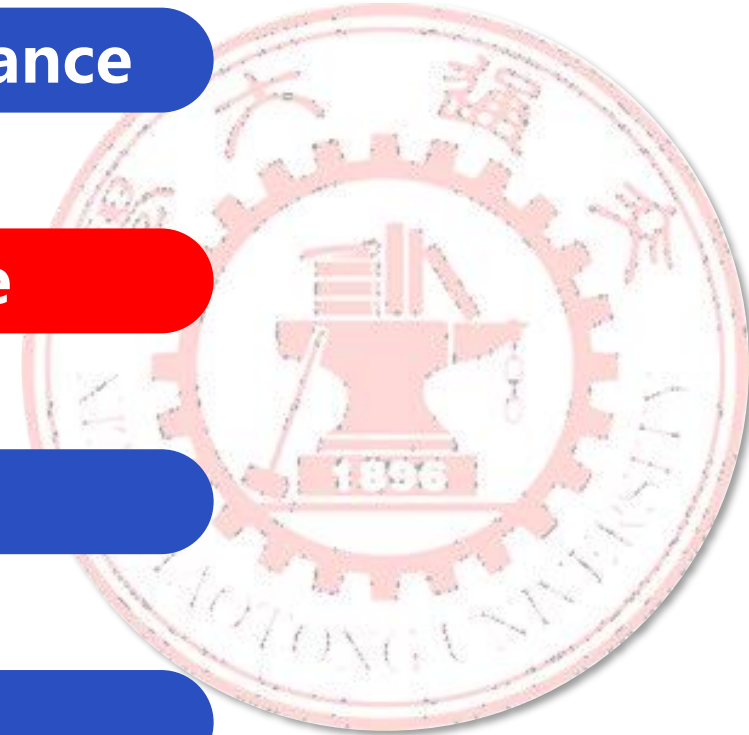
Complete the “Lockheed” semi-empirical equation of flame-retardant MLI (aluminum foil + glass fiber paper) based on the experimental results.

Correlation fit

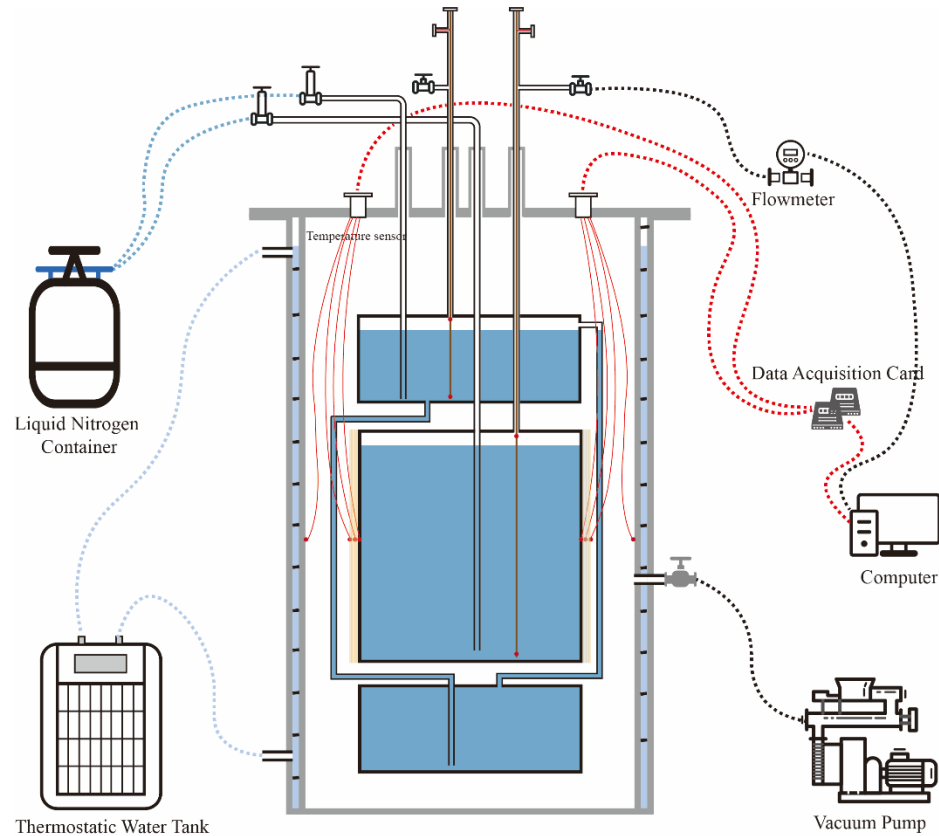


Content

- ① Research background and significance
- ② Experimental system and principle
- ③ Results and discussions
- ④ Conclusions and Suggestions



Experimental System Schematic Diagram



Capturing evaporated nitrogen mass flow.

$$Q = \dot{m}h_{fg}$$

Multilayer insulation structure



Aluminium Foil



Glass Fiber Paper



Combination



Wrap

LH₂ tanks multilayer insulation materials must be **flame retardant.**

Reliability demonstration

Vacuum insulation (no insulation material wrapped)

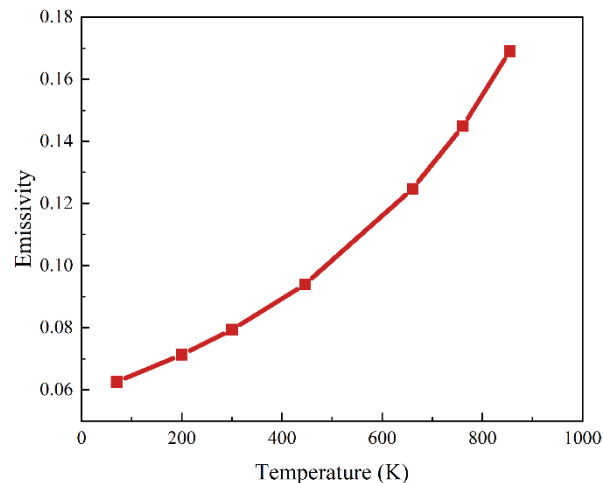
Vacuum pressure (Pa)	experimental pressure (kPa)	Warm boundary temperature (K)	Volume flow rate (L/min)	Heat leakage (W)	Heat flux (W/m ²)
3.95×10^{-3}	96.68	290.81	3.11	11.245	25.134

CINDAS LLC Data:

Slightly rough S316L emissivity

77 K → 0.0626

300 K → 0.0793



Heat flux **numerical** calculation:

$$q = \frac{\sigma(T_H^4 - T_C^4)}{\frac{1}{\epsilon_1} + \frac{A_1}{A_2} \left(\frac{1}{\epsilon_2} - 1 \right)} + C_1 \cdot P \cdot \alpha \cdot (T_H - T_C)$$

$$= 23.7 \text{ W/m}^2$$

Deviation: 1.434 W/m²
Relative Error: 5.71%

Heat flux of **different experimental systems** for vacuum insulation:

	Warm boundary temperature (K)	Cold boundary temperature (K)	Heat flux (W/m ²)
Ref. 1	297.15	77	48.140
Ref. 2	291.7	77	28.280
Ref. 3	283.15	77	26.894
This experiment	290.8	77	25.134 ★

Uncertainty analysis

Parameters of main measurement instruments

Parameter	Instrument	Range	Accuracy
P	Pressure sensor	0-100 kPa (a)	0.05% FS
T	Lackshore Cernox Thermometer	3.8-325 K	0.1 K
L, D	Meter rule	0-5 m	0.001 m
m	Alicat DB9 Flowmeter	0-5 NLPM 0-500 SCCM	0.1% FS



Apparent thermal conductivity:

$$k_{\text{eff}} = \frac{Q \cdot \ln(d_0 / d_i)}{2\pi L \cdot \Delta T}$$

Relative error:

$$\frac{\sigma k_{\text{eff}}}{k_{\text{eff}}} = \sqrt{\left(\frac{\sigma Q}{Q}\right)^2 + \left(\frac{\sigma(d_0 / d_i)}{(d_0 / d_i) \cdot \ln(d_0 / d_i)}\right)^2 + \left(\frac{\sigma L}{L}\right)^2 + \left(\frac{\sigma T}{T}\right)^2}$$

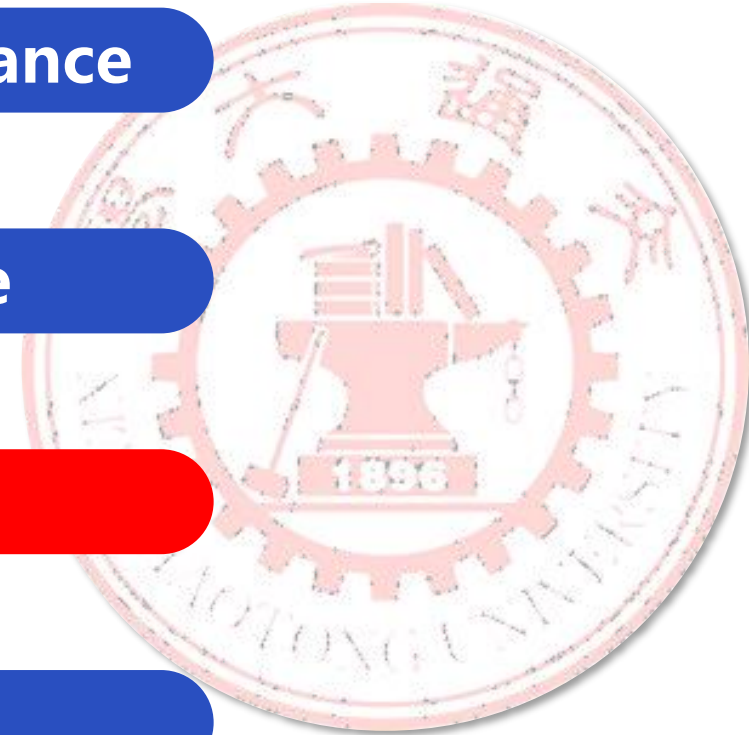
The experimental section **diameter** provides a large error

➤ Increase the experimental section's diameter

	Experimental section diameter (mm)	Experimental section height (mm)	Uncertainty
Ref. 4	200	400	3.4%
Ref. 5	200	300	3.2%
Ref. 6	152	375	3.31%
Ref. 7	100	450	3.73%
This experiment	350	400	1.34%

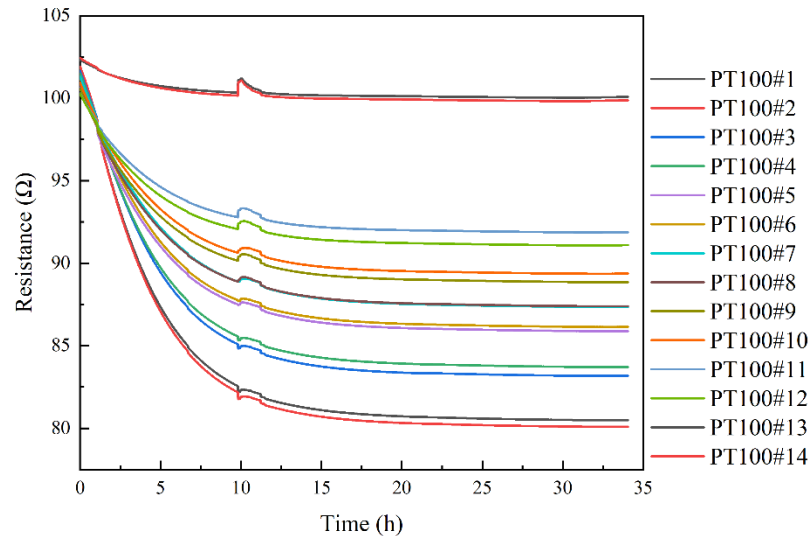
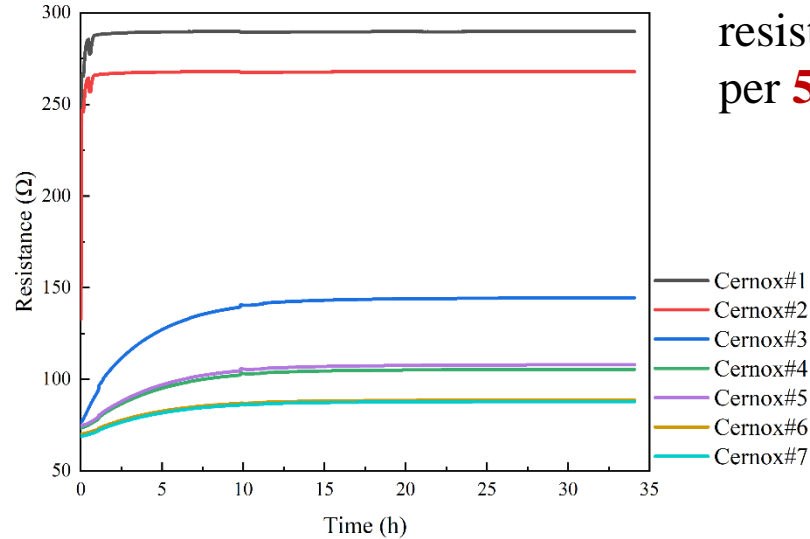
Content

- ① Research background and significance
- ② Experimental system and principle
- ③ Results and discussions
- ④ Conclusions and Suggestions

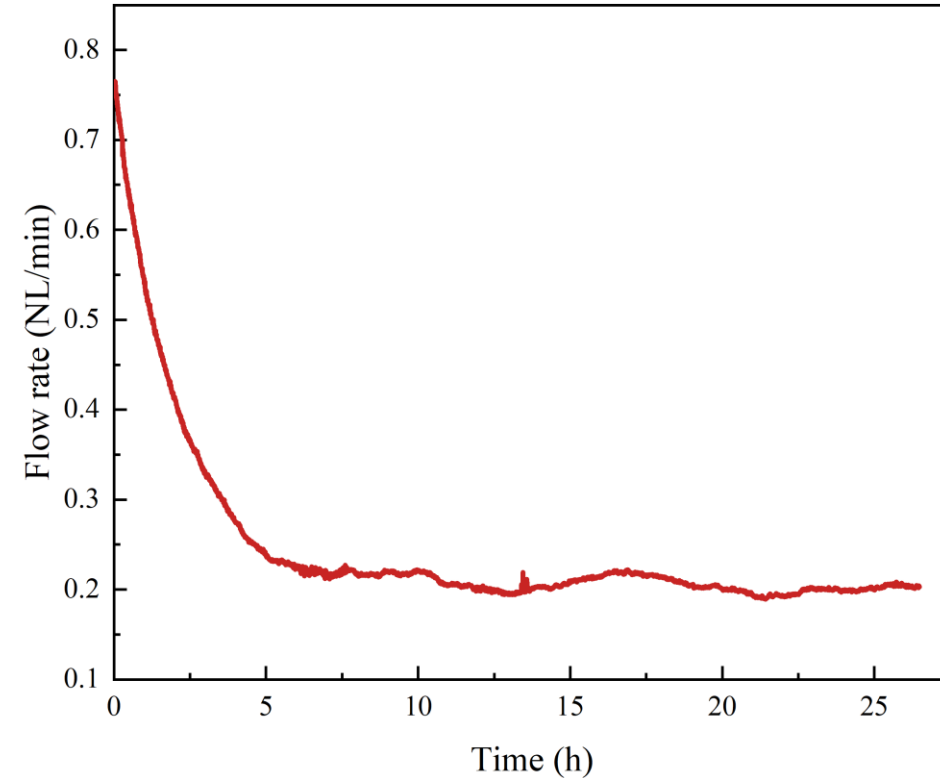


Data stabilization

Two platinum resistors arranged per **5** layers.



4-wire Resistance

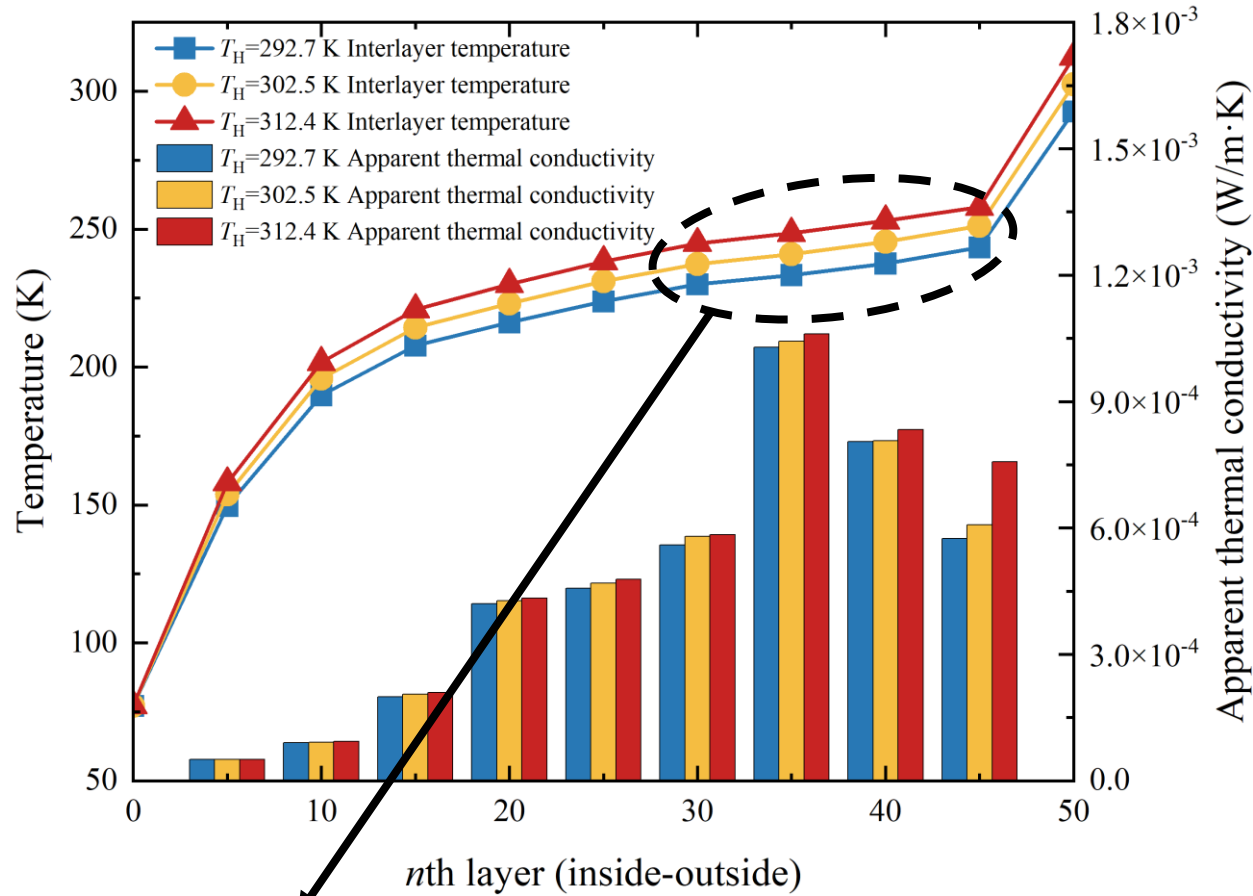


Data stabilized for **5 h** before starting data acquisition

Volume flow rate

- Maximum: 0.208 NL/min
- Minimum: 0.19 NL/min
- Average: **0.199 NL/min**

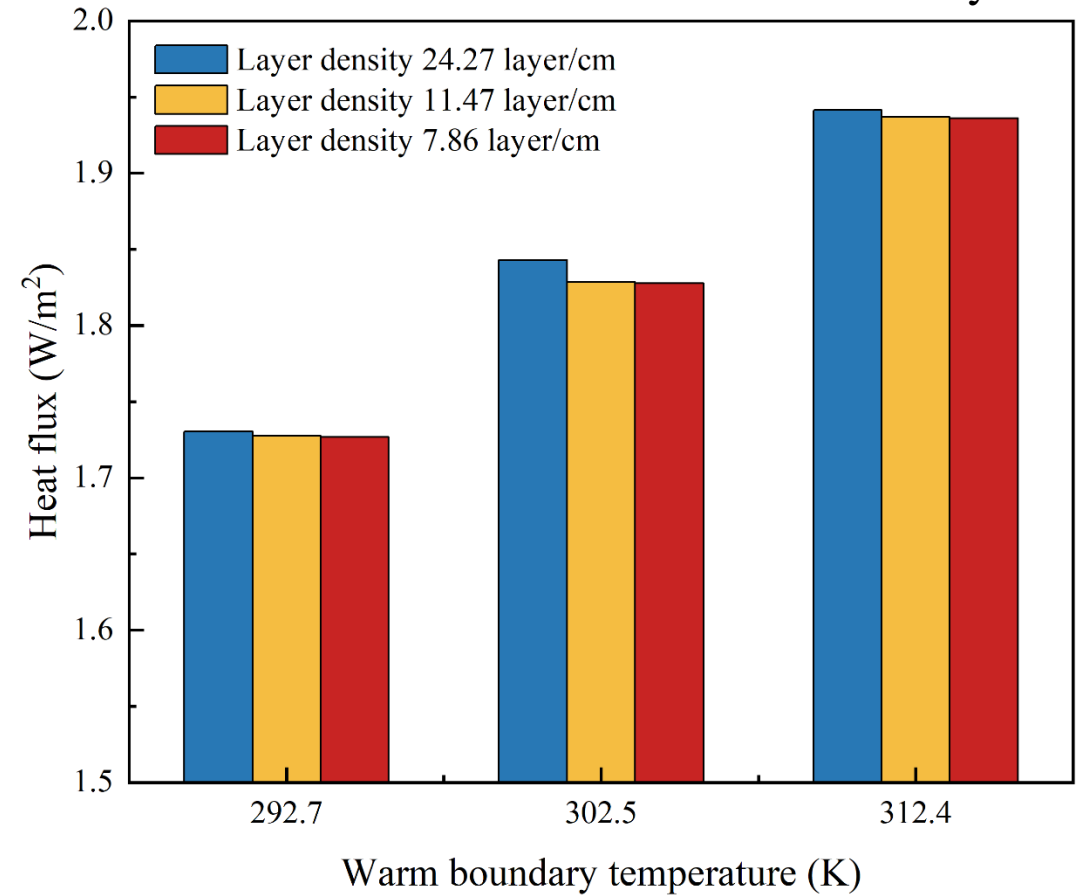
Rehydration at 12 h intervals in the protection section also affects the experimental section.



Minimum interlayer temperature differences occur in layers **30-35** rather than 40-45.

The vacuuming efficiency is the worst in the **middle** insulation structure, where the interlayer vacuum pressure is high.

Constant radiation shield layers



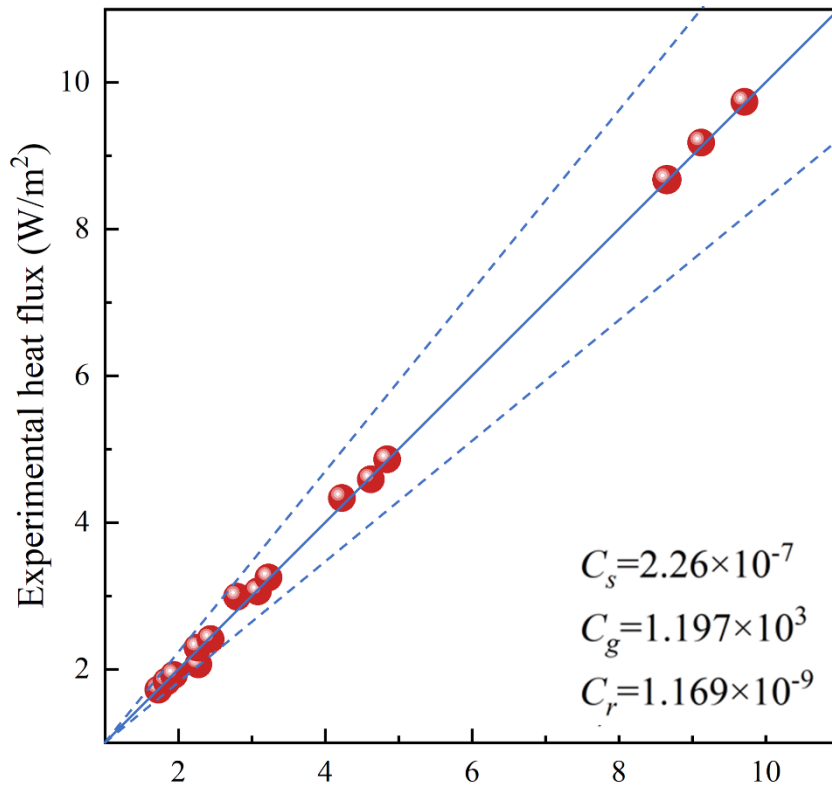
The layer density decreases, making the heat flux decrease.

Warm boundary temperature	292.7 K	302.5 K	312.4 K
Apparent thermal conductivity	1.86×10^{-4} W/(m·K)	1.89×10^{-4} W/(m·K)	1.91×10^{-4} W/(m·K)

Semi-empirical “Lockheed” Equation

$$q = \frac{C_s (n^*)^{2.63} (T_H - T_C)(T_H + T_C)}{2(n_s + 1)} + \frac{C_r \varepsilon (T_H^{4.67} - T_C^{4.67})}{n_s} + \frac{C_g p (T_H^{0.52} - T_C^{0.52})}{n_s}$$

C_s , C_g , and C_r are **coefficients** for solid conduction, gas conduction, and radiation heat transfer.



Predicting heat flux (W/m²)

Maximum deviation: **0.19 W/m².**

Average relative deviation: **1.74%.**

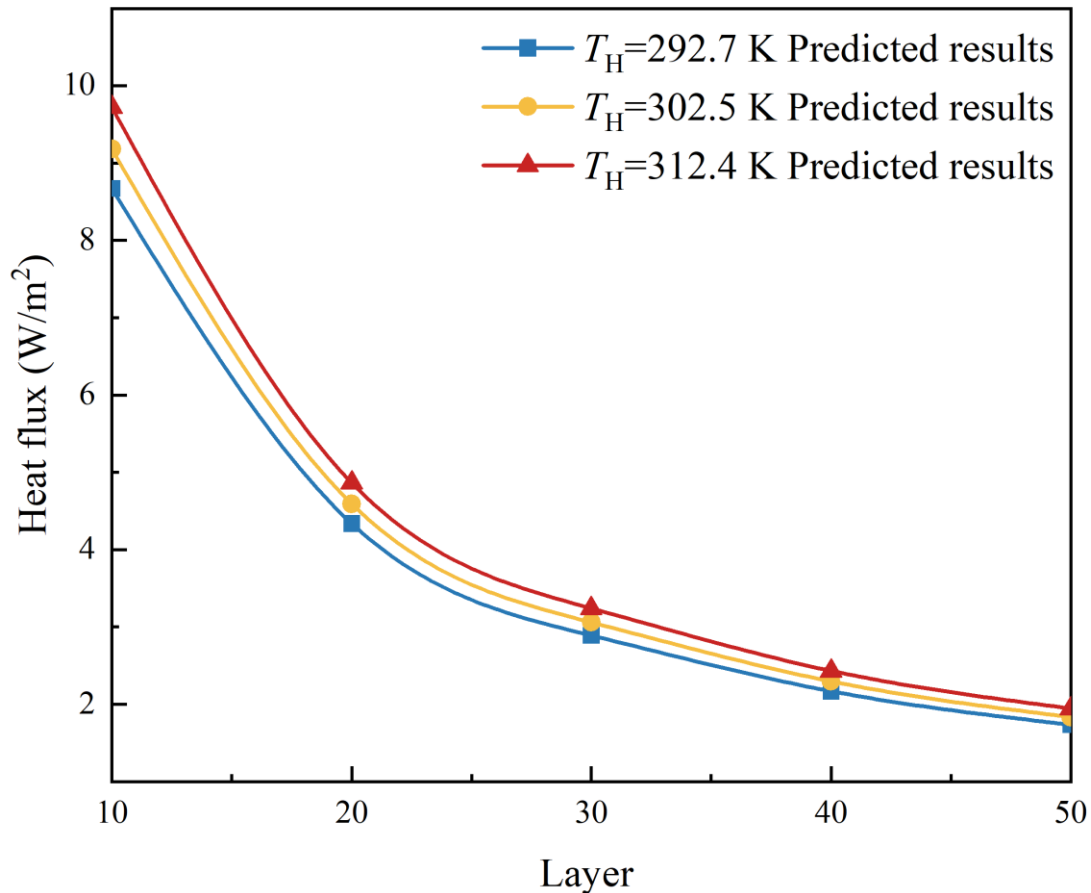
$$k = q \frac{\delta}{(T_H - T_C)}$$

$$k = \frac{C_s (n^*)^{2.63} (T_H + T_C) \delta}{2n_s} + \frac{C_r \varepsilon \sigma (T_H^{4.67} - T_C^{4.67}) \delta}{n_s (T_H - T_C)} + \frac{C_g \cdot p (T_H^{0.52} - T_C^{0.52}) \delta}{n_s (T_H - T_C)}$$

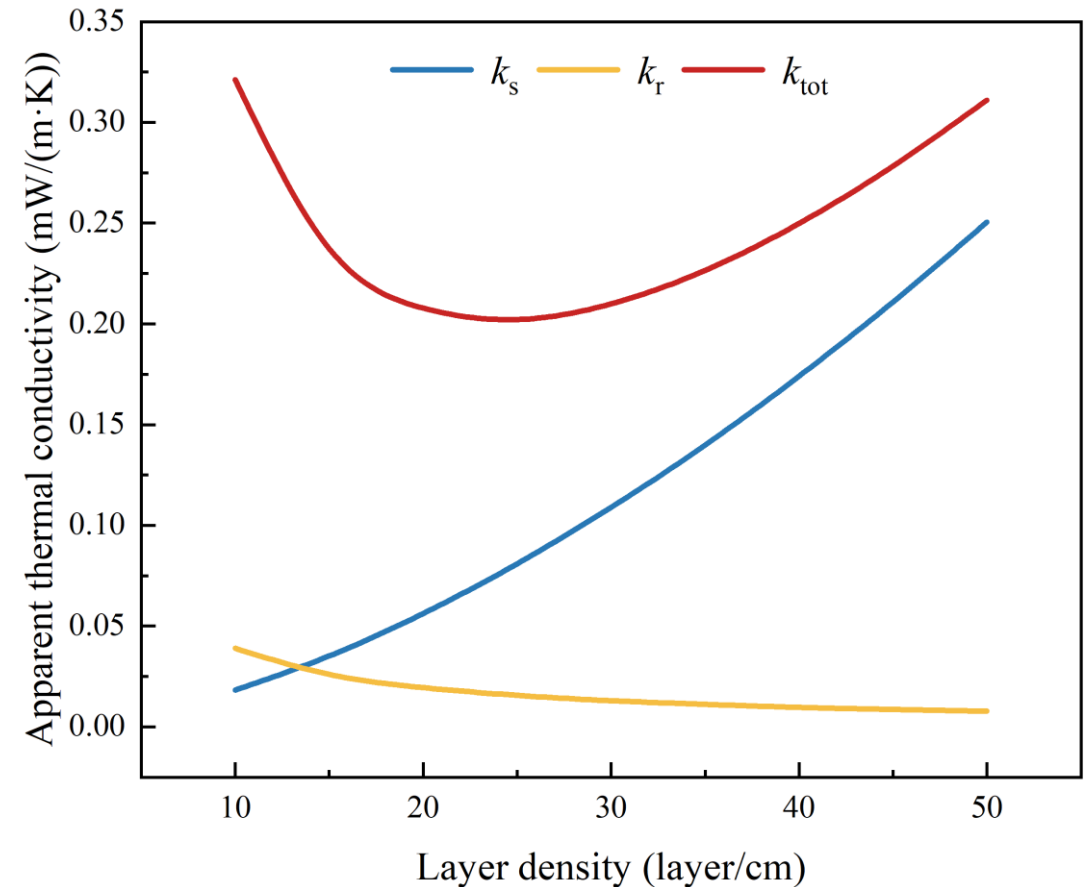
$$N_{OPT}^* = \left[\frac{C_r \varepsilon (T_H^{4.67} - T_C^{4.67}) + C_g p (T_H^{0.52} - T_C^{0.52})}{0.815 C_s (T_H^2 - T_C^2)} \right]^{\frac{1}{2.63}}$$

Optimal layer density: **$N_{OPT}=23$ Layer/cm**

Constant layer density



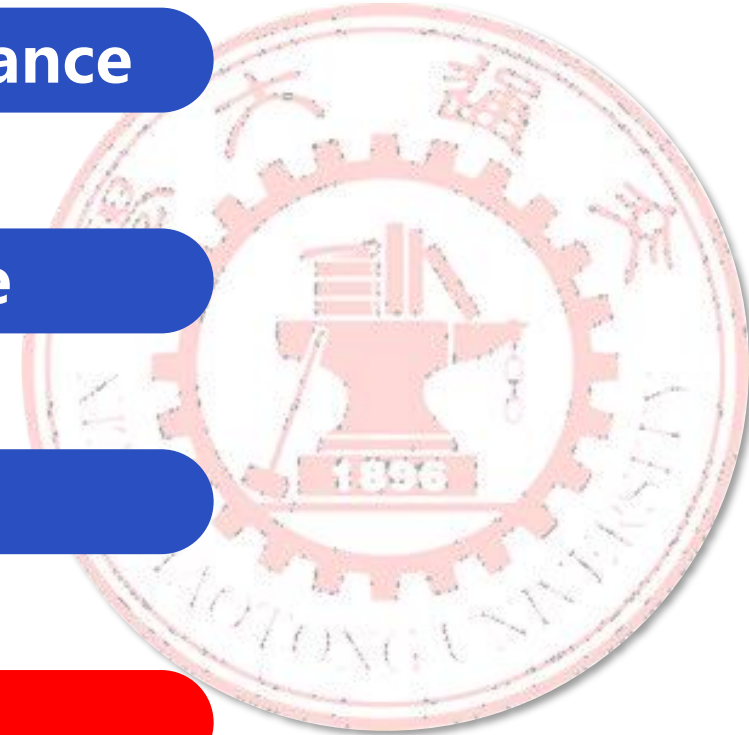
- **Too few radiation shield layers** cannot achieve an excellent insulation effect.
- Due to the low permeability of aluminum foil, **too many layers** can make vacuuming between MLI layers more difficult.



- The **gas and radiation** apparent thermal conductivity **decreases** with increasing layer density.
- The **solid** apparent thermal conductivity **increases** with increasing layer density.

Content

- ① Research background and significance
- ② Experimental system and principle
- ③ Results and discussions
- ④ Conclusions and Suggestions



1

The diameter of the experimental section causes a larger error than other parameters, and it is necessary to increase the diameter of the experimental section in the design.

2

The heat leakage of multilayer insulation structures decreases with the decrease of layer density, but this decreasing tendency is gradually weakened. The heat leakage is positively correlated with the warm boundary temperature.

3

The fitted equation can better predict the multilayer insulation structures (aluminum foil and glass fiber paper) heat leakage with a maximum deviation of 0.19 W/m^2 and an average relative deviation of 1.74%.



西安交通大学
XI'AN JIAOTONG UNIVERSITY

Thank you

Reporter: Hongyu Lv

Advisor: Professor Liang Chen

Thank the following for their support and guidance in this research:

- National Key Research and Development Program of China
(No. 2022YFB4002900)
- MOE key Laboratory of cryogenic technology and equipment

2024.07.24